

Local Discontinuous Galerkin Method for Modified Buckley-Leverett Equation

Lijuan Ma

College of Science, University of Shanghai for Science and Technology, Shanghai, China
 malijuan13@163.com

Abstract. This paper develops a local discontinuous Galerkin (LDG) method based on generalized numerical fluxes for solving traveling wave solutions of the modified Buckley-Leverett equation. To achieve efficient computation, the original equation is reformulated into a first-order system by introducing auxiliary variables, followed by spatial discretization using the DG method, while the explicit third-order Runge-Kutta method is adopted for temporal discretization. Based on the antisymmetry of the discrete spatial operator, the stability of the scheme under the energy norm is rigorously established. Numerical experiments demonstrate the robustness of the proposed method in handling convection-dominated problems with Riemann initial data, confirming its capability to accurately capture the shock structures.

Keywords: Local discontinuous Galerkin method, modified Buckley-Leverett equation, stability analysis, generalized numerical fluxes

1. Introduction

We focus on solving the modified Buckley-Leverett (MBL) equation with homogeneous boundary conditions [1] that models two-phase flow in porous media with dynamic capillary pressure effects [2]

$$U_t + f(U)_x = \varepsilon U_{xx} + \varepsilon^2 \mu U_{xxt}, x \in \Omega = (0, 3) \quad (1)$$

where constants $\varepsilon, \mu \geq 0$ denote the viscosity and dynamic capillary pressure coefficients, respectively. The nonlinear flux function f is defined as

$$f(U) = \begin{cases} 0, & U < 0, \\ \frac{U^2}{U^2 + M(1-U)^2}, & M > 0, 0 \leq U \leq 1 \\ 1, & U > 1 \end{cases} \quad (2)$$

where $M = 1/2$ denotes the mobility ratio between the two phases. The third-order mixed derivative term $\varepsilon^2 \mu U_{xxt}$ accounts for dynamic capillary pressure effects, essential for explaining saturation overshoot phenomena. We consider the Riemann initial condition $U_0 = U_B$ for $x \in (3/4, 9/4)$; otherwise, $U_0 = 0$, where $U_B \in (0, 1]$ denotes the injection saturation.

Theoretical analysis of the MBL equation has been extensively studied. Van Duijn et al. [3] revealed that the traveling wave solution profiles of this equation depend on the Riemann initial value parameters and the coefficients of high-order terms, including classical shocks, non-classical undercompressive shocks, and oscillatory profiles. Further theoretical developments include global existence results [4], shock wave admissibility criteria [5], uniqueness of weak solutions [6], and adaptive mesh investigations [7].

Various numerical methods for pseudo-parabolic equations include finite difference and Eulerian-Lagrangian methods [8], central schemes [9], and operator splitting methods [10]. Theoretical error estimates have also been established for relevant problems, covering local discontinuous Galerkin (LDG) methods [11,12], spectral methods [13], and upwinding strategies [14]. However, all these convergence results rely on the assumption that exact solutions are sufficiently smooth. For non-smooth initial data, optimal convergence may fail, especially for convection-dominated equations, which may exhibit physical oscillations or even non-convergence.

Based on this, this paper constructs an LDG method with generalized numerical fluxes for the convection-dominated MBL equation under Riemann initial data. The goal is to enhance numerical stability and computational effectiveness, particularly in capturing sharp discontinuities and suppressing spurious oscillations. Its key highlight is introducing properly designed auxiliary variables and exploiting their intrinsic spatial-temporal derivative transformation relationships, enabling high-order explicit time marching of the decoupled system and significantly improving computational efficiency.

The remainder of this paper is organized as follows. Section 2 presents the LDG scheme and its stability analysis. Section 3 presents numerical experiments. Finally, Section 4 makes some conclusions.

2. LDG method and stability analysis

2.1. Notations

Let $\Omega_h = \{I_j = (x_{j-1/2}, x_{j+1/2})\}$ be a partition of a given domain Ω . Denote the cell length as $h_j = x_{j+1/2} - x_{j-1/2}, j = 1, 2, \dots, N$, and $h_j = \max_j\{h_j\}$. We assume Ω_h is a quasi-uniform mesh in this paper, namely, there exists a fixed positive constant v independent of h , such that $vh \leq h_j \leq h$ for any j , as $h \rightarrow 0$.

The discontinuous finite element space is $V_h = \{v(x) : v|_{I_j} \in P_k(I_j), \forall j\}$, where $P_k(I_j)$ denotes the space of polynomials of degree at most $k \geq 0$. At each interface $x_{j+1/2}$, we define $\llbracket v \rrbracket_{j+1/2} = v_{j+1/2}^+ - v_{j-1/2}^-$ and $\{\{v\}\}_{j+1/2}^\beta = \beta v_{j+1/2}^- + (1 - \beta) v_{j+1/2}^+$, where $v_{j+1/2}^\pm = \lim_{x \rightarrow x_{j+1/2}^\pm} v(x)$ are one-sided limits and β is a given weight.

2.2. Semi-discrete LDG scheme

Introducing auxiliary variables $W = U_t, P = W_x, Q = U_x$, equation (1) is rewritten as two first-order differential systems where time and space variables are completely decoupled:

$$U_t = W, Q_t = P, W + (f(U) - \varepsilon Q - \varepsilon^2 \mu P)_x = 0, P = W_x \quad (3)$$

The semi-discrete LDG scheme seeks $z(t) = (z_{uq}, z_{wp}) = (u, q, w, p) \in (V_h)^4$ such that

$$(u_t, v_u) = (w, v_u), (q, v_q) = (p, v_q) \quad (4)$$

$$(w, v_w) - [H^f(u, v_w) - \varepsilon H^{1-\theta}(q, v_w) - \varepsilon^2 \mu H^{1-\theta}(p, v_w)] = 0 \quad (5)$$

$$(p, v_p) + H^\theta(w, v_p) = 0 \quad (6)$$

hold for any test functions $v_u, v_q, v_w, v_p \in V_h$. The DG discretizations are

$$H^\beta(\phi, \varphi) = \int_{\Omega_h} \phi \varphi_x dx + \sum_{j=1}^N \phi_{j+1/2}^\beta \llbracket \varphi \rrbracket_{j+1/2},$$

$$H^f(\phi, \varphi) = \int_{\Omega_h} f(\phi) \varphi_x dx + \sum_{j=1}^N \hat{f}(\phi)_{j+1/2} \llbracket \varphi \rrbracket_{j+1/2}.$$

We take the upwind-biased numerical flux $\hat{f}(u)_{j+1/2} = f(\{\{u\}\}^\theta)_{j+1/2}$ for nonlinear flux (2), and the generalized alternating fluxes $\hat{w} = \{\{w\}\}^\theta, \hat{p} = \{\{p\}\}^{1-\theta}, \hat{q} = \{\{q\}\}^{1-\theta}$ for high-order terms in (1)(referred as to generalized numerical fluxes). To ensure the stability of scheme, we take $\theta > 1/2$, since $f' \geq 0$ here.

The initial solutions $u_0 = P_h U_0(x)$ and $q_0 = P_h Q_0(x)$, where P_h denotes the local L^2 -projection. Until now, we have finished the definition of our scheme.

Theorem 1 (Stability). Let (u, q, w, p) be the solution of scheme (3-6). Define the energy norm $\|z_{uq}(t)\|^2 = \|u\|^2 + \varepsilon^2 \mu \|q\|^2$. Then, there holds for any $t \in (0, T]$ that $\|z_{uq}(t)\|^2 \leq \|z_{uq}(0)\|^2$

Proof. We proceed with the stability analysis in three steps.

Step 1: Derive the energy equation. Integrating (6) with respect to time over $(0, t]$ obtains that $(q, v_p) + H^\theta(u, v_p) = 0$. Choosing test functions $v_w = u, v_p = \varepsilon p$ and $v_p = \varepsilon^2 \mu p$, and collecting the obtained three identities, we yield:

$$\begin{aligned} & \frac{1}{2} \frac{d}{dt} \left[\|u\|^2 + \varepsilon^2 \mu \|q\|^2 \right] + \varepsilon \left[H^{1-\theta}(q, u) + H^\theta(u, q) \right] + \varepsilon^2 \mu \left[H^{1-\theta}(p, u) + H^\theta(u, p) \right] \\ &= H^f(u, u). \end{aligned}$$

Then, by using the antisymmetry property of DG discrete operator [15], namely: for any $\phi, \varphi \in H^1(I_h)$, and a given $\alpha \in \mathcal{R}$, there holds $H^{1-\alpha}(\phi, \varphi) + H^\alpha(\varphi, \phi) = 0$, we obtain the energy evolution equation: $\frac{1}{2} \frac{d}{dt} \left[\|u\|^2 + \varepsilon^2 \mu \|q\|^2 \right] = H^f(u, u)$.

Step 2: Prove non-positivity of $H^f(u, u)$. Define the entropy flux associated with the flux function $f(u)$ as $F(u) = \int_u f(s)ds$. Expand the semi-linear operator:

$$H^f(u, u) = \int_{\Omega_h} f(u)u_x dx + \sum_{j=1}^N \hat{f}(u)_{j+1/2} \llbracket u \rrbracket_{j+1/2} = - \sum_{j=1}^N \llbracket F(u) \rrbracket_{j+1/2} + \sum_{j=1}^N \hat{f}(u)_{j+1/2} \llbracket u \rrbracket_{j+1/2}.$$

where we have used the homogeneous boundary conditions. For any interface, let $z = \theta u^- + (1 - \theta)u^+$. Since $f' \geq 0$, $f(z)$ lies between $f(u^-)$ and $f(u^+)$. Using the non-convexity of f and the integral mean value inequality, we analyze two cases:

If $u^+ \geq u^-$: As f is non-decreasing and $\theta > 1/2$, the non-convexity of f implies $f(z) \leq \frac{1}{u^+ - u^-} \int_{u^-}^{u^+} f(s)ds = \llbracket F(u) \rrbracket$. Multiplying both sides by $u^+ - u^- \geq 0$ preserves the inequality: $f(z)(u^+ - u^-) \leq \int_{u^-}^{u^+} f(s)ds$

If $u^+ < u^-$: Rewrite the integral as $\int_{u^-}^{u^+} f(s)ds$ and use $f(z) \leq \frac{1}{u^+ - u^-} \int_{u^-}^{u^+} f(s)ds$. Multiplying by $u^+ - u^- = -(u^- - u^+)$ (reversing the inequality once) and noting $\int_{u^-}^{u^+} f(s)ds = - \int_{u^+}^{u^-} f(s)ds$, we still obtain: $f(z)(u^+ - u^-) \leq \int_{u^-}^{u^+} f(s)ds = \llbracket F(u) \rrbracket$.

Thus, we obtain $H^f = - \sum_j \llbracket F(u) \rrbracket_{j+1/2} + \sum_j \hat{f}_{j+1/2} \llbracket u \rrbracket_{j+1/2} \leq 0$.

Step 3: Final energy estimate. Substituting $H^f \leq 0$ into the energy equation gives $\frac{d}{dt} \|z_{uq}(t)\|^2 \leq 0$.

3. Numerical experiments

In (1), we consider $\varepsilon = 10^{-3}$. We investigate the effects of flux parameter $\theta = 0.7, 1.0, 1.3$ and polynomial degree $k = 1, 2, 3$. We use the LDG method to compute the solution at the final time $T = 0.5$.

Effect of θ : We fix $k = 3$ and investigate the solution characteristics corresponding to different θ values. According to the traveling wave solution theory in [3], when $(\mu, u_B) = (5, 0.52)$, the exact solution includes a non-monotone plateau in the right portion. The numerical solution obtained by our LDG method with $N = 512$, as shown in Fig. 1, agrees well with the exact solution in terms of its form. Similarly, when $(\mu, u_B) = (5, 0.66)$, the theory in [3] indicates that the exact solution includes a non-monotone plateau in the right part. Our numerical results, as shown in Fig. 2 for $N = 512$, clearly delineate the theoretical characteristics of the aforementioned exact solution. All solutions exhibit a non-monotone plateau on the right. From these results, it can be observed that the influence of θ is not significant. Thus, for simplicity, we choose $\theta = 1$ in subsequent computations.

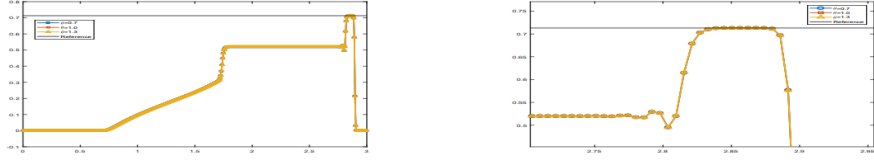


Figure 1. Solutions corresponding to $(\mu, u_B) = (5, 0.52)$, calculated by the LDG method (where $\theta = 0.7, 1.0, 1.3, N = 512$) (Left: full view; Right: close-up view of the platform area)

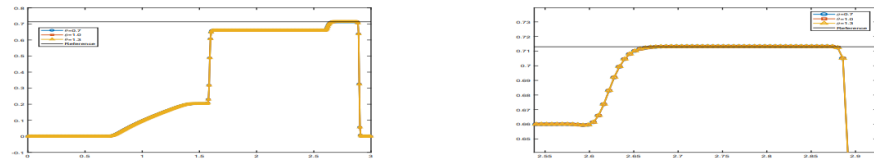


Figure 2. Solutions corresponding to $(\mu, u_B) = (5, 0.66)$, calculated by the LDG method (where $\theta = 0.7, 1.0, 1.3, N = 512$) (Left: full view; Right: close-up view of the plateau area)

Effect of k : Next, we demonstrate the LDG method's numerical performance for piecewise polynomials. To verify the scheme's accuracy, we check predicted plateau height and shock location via mesh refinement. In [16], for (specific parameter), the exact solution's right portion jumps to a plateau then back to 0, plus damped oscillations near (parameter)—features a well-designed scheme should capture. Fig. 3 shows higher-order polynomial-based numerical solutions capture these features more accurately. In Fig. 3, we can see that numerical solutions based on higher-order polynomials are able to capture these key features with greater accuracy. Moreover, theoretical analysis indicates that when $u_B = 0.66$, the width of the plateau region \tilde{u}^f of the corresponding solution increases, and the wavefront oscillations gradually vanish. As illustrated in Fig. 4, the LDG solutions can accurately capture the profile of the theoretical traveling wave solutions.

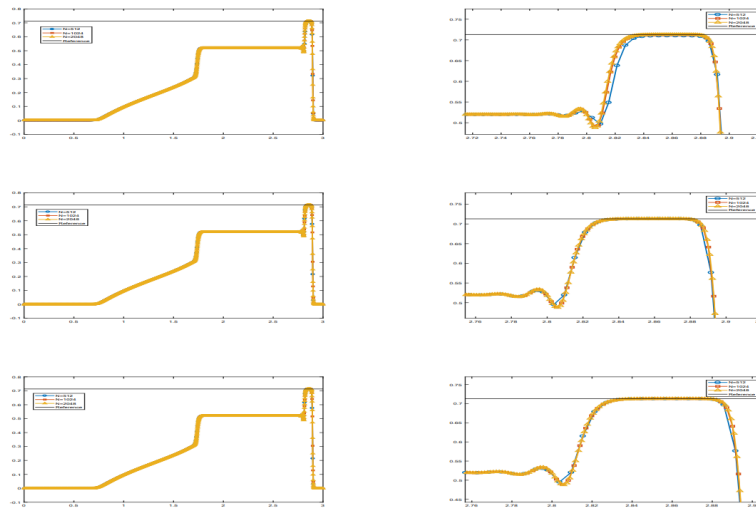


Figure 3. Solutions corresponding to $(\mu, u_B) = (5, 0.52)$, calculated by the LDG method with $\theta = 1.0, N = 512, 1024, 2048$, from top to bottom, respectively $k = 1, 2, 3$ (Left: full view; Right: plateau close-up)

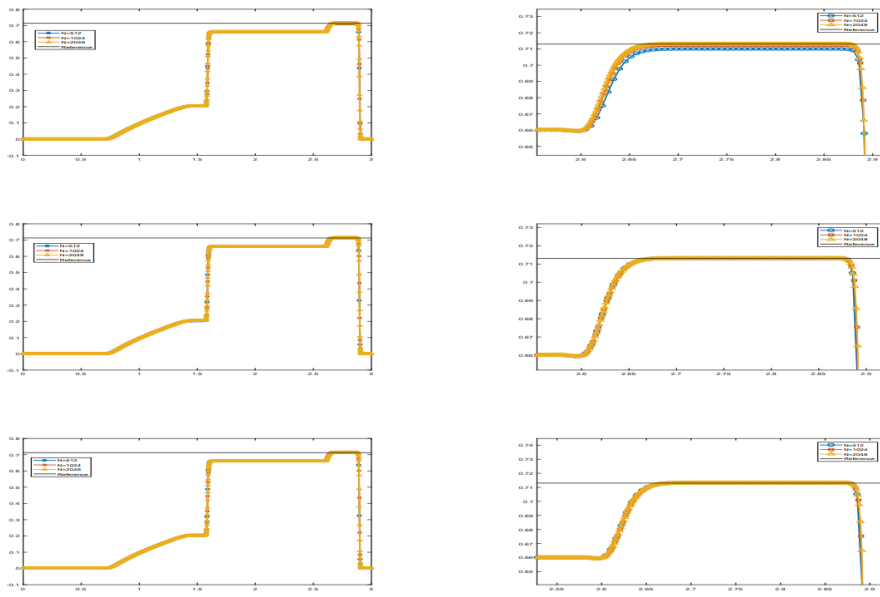


Figure 4. Solutions corresponding to $(\mu, u_B) = (5, 0.66)$, calculated by the LDG method with $\theta = 1.0, N = 512, 1024, 2048$, from top to bottom, respectively $k = 1, 2, 3$ (Left: full view; Right: plateau close-up)

4. Conclusion

We developed an LDG method with generalized numerical fluxes for solving the MBL equation accounting for dynamic capillary pressure. The equation's pseudo-parabolic nature (involving mixed space-time derivatives) complicates discretization and stability analysis, so we designed auxiliary variables to decompose it into two fully decoupled first-order linear systems—simplifying numerical implementation and enabling rigorous stability analysis. Leveraging the antisymmetric structure of DG discretization, we proved the semi-discrete scheme's stability under the energy norm. Numerical experiments show the method effectively captures complex wave structures like non-monotone plateaus and shocks. Future work will focus on error analysis for non-smooth data and adaptive strategies for convection-dominated cases.

References

- [1] C.V. Duijn, S. Hassanzadeh, I. Pop and P. Zegeling, et al., Non-equilibrium models for two phase flow in porous media: the occurrence of saturation overshoots, In: CAPM 2013-Proceedings of the 5th International Conference on Applications of Porous Media, (2013), 59-70.
- [2] S.M. Hassanzadeh, W.G. Gray, Thermodynamic basis of capillary pressure in porous media, Water Resour. Res., 29 (1993), 3389-3405.
- [3] C.V. Duijn, L. Peletier, I. Pop, A new class of entropy solutions of the Buckley-Leverett equation, SIAM J. Math. Anal., 39 (2007), 507-536.
- [4] A. Mikelic, A global existence result for the equations describing unsaturated flow in porous media with dynamic capillary pressure, J. Differ. Equ., 248 (2010), 1561-1577.
- [5] K. Spayd, M. Shearer, The Buckley-Leverett equation with dynamic capillary pressure, SIAM J. Appl. Math., 71 (2011), 1088-1108.
- [6] X. Cao, I. Pop, Uniqueness of weak solutions for a pseudo-parabolic equation modeling two phase flow in porous media, Appl. Math. Lett., 46 (2015), 25-30.

- [7] H. Zhang, P.A. Zegeling, Numerical investigations of two-phase flow with dynamic capillary pressure in porous media via a moving mesh method, *J. Comput. Phys.*, 345 (2017), 510-527.
- [8] R.D.O. Garcia, G.P. Silveira, Numerical solutions of the classical and modified Buckley-Leverett equations applied to two-phase fluid flow, *Open J. Fluid Dyn.*, 14 (2024), 184-204.
- [9] Y. Wang, C.Y. Kao, Central schemes for the modified Buckley-Leverett equation, *J. Comput. Sci.*, 4 (2013), 12-23.
- [10] F. Zhang, L. Nghiem, Z. Chen, A novel approach to solve hyperbolic Buckley-Leverett equation by using a transformer based physics informed neural network, *Geoenergy Sci. Eng.*, 236 (2024), 212711.
- [11] F.Z. Gao, J.X. Qiu and Q. Zhang, Local discontinuous Galerkin finite element method and error estimates for one class of Sobolev equation, *J. Sci. Comput.*, 3 (2009), 436-460.
- [12] D. Zhao and Q. Zhang, Local discontinuous Galerkin methods with generalized alternating numerical fluxes for two-dimensional linear Sobolev equation, *Journal of Scientific Computing*, (2019), 1-31.
- [13] X. Yu and M. Wang, Efficient spectral and spectral element methods for Sobolev equation with diagonalization technique, *Appl. Numer. Math.*, 201 (2024), 265-281.
- [14] S. Jayasinghe et al., Upwinding and artificial viscosity for robust discontinuous Galerkin schemes of two-phase flow in mass conservation form, *Comput. Geosci.*, 25 (2021), 191-214.
- [15] C. Du, D. Zhao, Q. Zhang, Error estimate of high order Runge-Kutta local discontinuous Galerkin method for nonlinear convection-dominated Sobolev equation, *J. Comput. Appl. Math.*, 469 (2025), 116657.
- [16] C.Y. Kao, A. Kurganov, Z. Qu, Y. Wang, A fast explicit operator splitting method for modified Buckley-Leverett equations, *J. Sci. Comput.*, 64 (2015), 837-857.